Plant Physiology and Biochemistry 118 (2017) 245–255

Contents lists available at ScienceDirect

Plant Physiology and Biochemistry

journal homepage: www.elsevier.com/locate/plaphy

Research article

Comparative proteomic and metabolomic studies between *Prunus persica* genotypes resistant and susceptible to *Taphrina deformans* suggest a molecular basis of resistance

Camila Goldy [a, 1, 3], Laura A. Svetaz [a, 1, 2], Claudia A. Bustamante [a], Marco Allegrini [a, 4], Gabriel H. Valentini [b], María F. Drincovich [a], Alisdair R. Fernie [c], María V. Lara [a, *]

[a] Centro de Estudios Fotosintéticos y Bioquímicos (CEFOBI, Consejo Nacional de Investigaciones Científicas y Técnicas (CONICET)), Facultad de Ciencias Bioquímicas y Farmacéuticas (FCByF), Universidad Nacional de Rosario (UNR), Suipacha 531, 2000, Rosario, Argentina
[b] Estación Experimental San Pedro, Instituto Nacional de Tecnología Agropecuaria (INTA), Ruta Nacional nº 9 Km 170, San Pedro, Argentina
[c] Max-Planck-Institut für Molekulare Pflanzenphysiologie, Am Mühlenberg 1, 14476, Potsdam-Golm, Germany

ARTICLE INFO

Article history:
Received 28 April 2017
Received in revised form
2 June 2017
Accepted 16 June 2017
Available online 17 June 2017

Keywords:
Dimorphism
Biotroph
Proteomics
Metabolomics
β-Glucanase
Lipid-transfer protein
Thaumatin-like protein
Bet-v1-like
Chlorogenic acid

ABSTRACT

The worldwide-distributed leaf peach curl disease is caused by the biotroph *Taphrina deformans*. To characterize the plant-fungus interaction, resistant and susceptible *Prunus persica* genotypes grown in the orchard were studied. Asymptomatic leaves were tested for fungal presence. In all resistant leaves analyzed the fungus was not detected. Conversely, leaves from the susceptible genotype were categorized according to the presence or absence of the pathogen.

Comparative metabolomic analysis disclosed the metabolite composition associated with resistant and susceptible interactions, and of compounds involved in fungal growth inhibition such as chlorogenic acid, whose *in vitro* antifungal activity was verified in this work.

Differential proteome studies revealed that chloroplasts are important site of plant defense responses against *T. deformans*. Members of the Bet-v1-like family protein differentially responded to the pathogen. Extracellular pathogenesis-related proteins, evaluated by qRT-PCR, and an enone oxidoreductase are constitutively present in leaves of resistant trees and could be related to fungal resistance.

This study is a global view of the changes in the metabolome, proteome and transcripts related to plant defense in naturally infected leaves of susceptible plants during the asymptomatic stage. Additionally, it provides clues to the successful molecular mechanisms operating in resistant plants, which neither develop the disease nor harbor the pathogen.

1. Introduction

Prunus persica L. (Batsch) is a model species for the Rosaceae family (Shulaev et al., 2008). It is the third temperate fruit in cultivated surface area, and its production is of great economic importance. Its genome has been sequenced, and many resources are available enabling progress in the study of the inheritance of many major genes with impact on fruits, tree architecture, flower morphology and disease resistance (Arús et al., 2012).

Among different pathogens infecting peach trees, the fungus *Taphrina deformans* is responsible for leaf curl disease. Under severe infections, twigs, flowers and fruits are attacked. Leaf curl disease of stone fruit trees is distributed in virtually all fruit growing regions of the world (Fonseca and Rodrigues, 2011). Typical symptoms of the disease, which are evident across spring and summer seasons,

Abbreviations: CAT, catalase; Gns4, β-1,3-endoglucanase; 2-DE, two-dimensional PAGE; DFN, Defensin; DR, DOFI- 84.364.060; DS, DOFI-84.364.089; GABA, 4-amino-butyrate; LTP, Lipid-Transfer Protein; PAL, Phenylalanine Ammonia Lyase; PC, principal component; PCA, principal component analysis; PR, pathogenesis-related; TLP, Thaumatin-Like Protein.

* Corresponding author.
E-mail address: lara@cefobi-conicet.gov.ar (M.V. Lara).

[1] Both authors contributed equally to this work.
[2] Present address: Farmacognosia, FCByF, UNR.
[3] Present address: Instituto de Biología Molecular y Celular de Rosario (IBR-CONICET), FCByF, UNR, Argentina.
[4] Present address: Instituto de Investigaciones en Ciencias Agrarias Rosario (IICAR-CONICET). Laboratorio de Biodiversidad Vegetal y Microbiana, UNR, Campo Experimental J. Villarino, 2125 Zavalla, Argentina.

http://dx.doi.org/10.1016/j.plaphy.2017.06.022
0981-9428/

include leaves that curl inward and downward and are intensively distorted, wrinkled and thickened. The initial sign of the disease is the change in the color firstly pale green or yellow and subsequently to reddish or purplish (Fonseca and Rodrigues, 2011). *T. deformans* enters the host cells through the stomata (Svetaz et al., 2017). Light and electron-microscopic studies described the mycelial form of the fungus growing in the intercellular spaces and below the cuticle. *T. deformans* does not form haustorium; in contrast, the interface between the fungus and leaf cell wall is modified to enable fungal nutrition (Bassi et al., 1984). Modifications in the cell host anatomy have also been described during the infection (Giordani et al., 2013).

Rossi et al. (2007) studied the conditions favoring fruit and shoot infection, and established infection foretelling models (Giosuè et al., 2000). The risk of serious leaf curl outbreaks is high when wet and cold conditions are prolonged during bud development (Giosuè et al., 2000). Disease incidence being up to 89% for shoot and 50% for fruit under these conditions (Rossi et al., 2006, 2007). Severe attacks often lead to premature defoliation weakening tree vigour and diminishing fruit yield and quality (Rossi et al., 2007).

The high level of pesticides used annually to prevent this disease is concerning from the perspectives of the environment and human health. Thus, reduction of fungicide use is a priority for intensively sprayed agricultural systems such as orchards. In this context, the development of trees resistant to the pathogen is a sustainable alternative. Almost all commercial cultivars are susceptible (Simeone, 1987) with only a few being resistant to the pathogen (Scorza, 1992; Bellini et al., 2002; Zhivondov et al., 2016). A leaf curl resistance-breeding program started at the University of Florence in the 1990s generated a *T. deformans* resistant genotype (Bellini et al., 2002). Further studies identified that this resistance was a qualitative trait (Padula et al., 2008). The genotype DOFI-84.364.089 of the same program by contrast is susceptible to *T. deformans*.

In the current study, in order to gain insight into the molecular mechanisms involved in plant resistance to the disease, healthy leaves from both genotypes were compared to seek for differences in abundance of pre-existing proteins and metabolites that prevent the disease. Furthermore, to investigate the molecular responses of *P. persica* against *T. deformans* in early stages, when symptoms of the disease have not yet developed, leaves from susceptible DOFI-84.364.089 were classified according to whether the pathogen was present or absent and their metabolomes and proteomeswere analyzed. In addition, transcriptional analysis of pathogenesis-related (PR) and other proteins involved in defense mechanisms were conducted. Changes in transcripts, proteins and metabolites were interpreted in the context of their participation in the defense and infection processes. The combined data are discussed with regard to the ability of *P. persica* to deal with *T. deformans* and provide comprehensive data pertaining to the molecular mechanism(s) operating within this pathosystem.

2. Materials and methods

2.1. Plant material

Leaves of *Prunus persica* L. Batsch from the advanced selections DOFI-84.364.089 and DOFI-84.364.060, generated by breeding in University of Florence (Bellini et al., 2002), were harvested from plants grown at the Estación Experimental Agropecuaria INTA, San Pedro, Argentina, located at latitude S 33° 44′ 12.1″, longitude W 59° 47' 48.0". Regarding the pedigree of assayed genotypes, DOFI 84.364.060 and DOFI 84.364.089 belong to the progeny DOFI-84.364. This family was obtained by self-pollination of DOFI 71.043.018. In addition, DOFI 71.043.018 was generated from the self-pollination of cv. Cesarini ("Cesarini x Cesarini").

Plants of each genotype were monitored for at least five years and evaluated according the degree of infection. Selection DOFI-84.364.089 (DS) always resulted susceptible to *T. deformans* and DOFI-84.364.060 was resistant (DR). Leaves were collected and verified for integrity, absence of any lesions or signs of disease; that is, only healthy leaves were collected. Material was washed with sterile water, dried and individually frozen in $N_{2(l)}$ and kept at −80 °C.

Each leaf sample was homogenized in $N_{2(l)}$ using mortar and pestle. An aliquot of 100 mg was used for DNA extraction followed by *T. deformans* detection by PCR. Remaining material was employed for the rest of analysis.

2.2. Fungal detection in leaves of P. persica by PCR

Fungal DNA was extracted from leaves by using the modified CTAB method and glass beads, which simultaneously extracts DNA from leaf and fungus (Sampaio et al., 2001).

PCR detection of *T. deformans* was conducted amplifying the ITS1 region from fungal genomic DNA, which is the standard marker for fungal DNA barcoding (Chase and Fay, 2009), using TDITS1 forward (5′TCTCCGGATGGTTTCAA3′) and NL4 reverse primers (5′GGTCCGTGTTTCAAGACGG3′) (Tavares et al., 2004). Amplification was conducted as previously (Tavares et al., 2004) using a Px2 Thermal cycler (Thermo Electron Corporation). Tested DNA ranged between 20 and 80 ng. The quality of each sample was tested for putative PCR inhibitors by adding *T. deformans* DNA (20 ng) as internal control. Positive (*T. deformans* DNA) and negative (ddH_2O) amplification controls were run in each experiment. Reactions were performed, at least, twice. PCR products were analyzed on 1% (w/v) agarose gels stained with SYBR Safe (Invitrogen).

Control DNA was isolated from *T. deformans* strain (PYCC 5894, Portuguese Yeast Culture Collection, Lisboa, Portugal) grown as in Sampaio et al. (2001).

2.3. Metabolite measurements

Metabolite profiling was assessed by GC-MS following the procedures described in Roessner-Tunali et al. (2003) and in Monti et al. (2016), and employing 100 mg of leaf material. Ribitol was used as internal standard and methoxyamine hydrochloride in pyridine followed by *N*-methyl-*N*-[trimethylsilyl]trifluoroacetamide were employed for derivatization. Mass spectra were cross-referenced with those in the Golm Metabolome Database. Biological quintuplicates were analyzed. Data sets were subjected to principal component (PCA) and Pearson correlation analyses using XLSTAT package. Heat map was constructed using MultiExperiment Viewer software (MeV v4.4.1). Data was normalized and expressed as log2 ratios to DS-. Metabolite data was presented (Supplementary Table S1) according to Fernie et al. (2011).

2.4. Fungal growth inhibition

Leaf extracts were prepared from *P. persica* DS (11.9 g) and DR (13 g), freeze-dried, ground in mortar and extracted three-times with 150 ml methanol for 24 h at room temperature. Solvent evaporation under reduced pressure at 40 °C, gave 4.7 and 4.8 g of semisolid methanol extracts, respectively.

Micro-plate broth microdilution technique was performed (Rex et al., 2008). Chlorogenic acid and extracts were prepared with stock solutions in DMSO (≤1%) and diluted with RPMI-1640.

Inoculum suspension of 1–5. 10^4 CFU ml^{-1} was used. Growth (compound/extract-free) and sterility (inoculum-free) controls were included. Dicopper chloride trihydroxide was used as positive control. Microplates were incubated in a moist, dark chamber at 30 °C, 48 h and read in a VERSA Max microplate reader (Molecular Devices, CA, USA). Tests were performed in triplicate.

2.5. Pigment analysis

Carotenoids, chlorophylls, phenolic compounds and anthocyanins were quantified as in Svetaz et al. (2017). Briefly, carotenoids and chlorophylls were extracted in 96% (v/v) methanol during 24 h, clarified and spectrophotometrically measured. For phenolic compounds and anthocyanins extraction, 10 mg of fresh leaves were homogenated in the presence of N_2 (l) with 2 ml of 80% (v/v) acidic methanol (0.5 N HCl). After overnight incubation at 4 °C and clarification the supernatant was directly employed for anthocyanins quantification using spectrophotometry or for phenolics determination using the Folin reagent (Merck). A calibration curve was conducted using phenol as standard.

2.6. Differential proteome analysis

Protein extraction under denaturing conditions was conducted as in Lara et al. (2009) using the phenol method and 0.5 g of leaf.

Protein resuspension, quantification and labelling, and two-dimensional PAGE (2-DE) were conducted using the equipment and conditions described in Lara et al. (2009), 75 μg of Alexa 488 (Invitrogen)-labeled protein, precast immobilized pH 4–7 linear gradient strips (17 cm, Bio-Rad) and 15% (w/v) SDS-PAGE. To excise samples for MS analysis, a preparative gel loaded with 1 mg of protein was run.

For gel image analysis, Image Master 2D-Platinum (GE Healthcare) software was used as before (Lara et al., 2009). The differential proteome was assessed comparing leaves of DS in which *T. deformans* was confirmed by molecular methods *vs.* those in which the fungus was not detected (DS + *vs.* DS-). In addition, the proteome of DR that also resulted negative for the presence of the fungus (DR-) was contrasted with that of DS-. To obtain biological replicates, each sample was run in at least 3 different gels using different protein preparations from different leaves. Normalized spot volumes were compared between samples run in different gels. Difference thresholds were then applied to identify the proteins with a statistically significant 1.5-fold difference in normalized spot volume (*t*-test, $P < 0.05$).

In-gel digestion and MS were performed as previously described (Casati et al., 2006) using the matrix assisted laser desorption ionization time of flight MS (MALDI-TOF-TOF/MS) spectrometer, Ultraflex II (Bruker) from CEBIQUIEM facilities (FCEyN, UBA, Argentina). Data searching was conducted using MASCOT (Matrix Science Ltd.) and National Center for Biotechnology Information databases. Candidate peptides were considered as matches following the considerations described in Casati et al. (2006).

2.7. Gene expression analysis

RNA was extracted from 50 to 100 mg of leaves using the Trizol (Invitrogen) method and checked for integrity using agarose electrophoresis. The quantity and purity of RNA were assessed spectrophotometrically. Three micrograms of RNA, oligo(dT) and M-MLV-reverse transcriptase were used to synthesize first-strand cDNA following manufacturer's instructions (Promega, Madison, WI, USA).

Quantitative Real time- RT-PCR (qRT-PCR) was used to evaluate gene expression using a MiniOpticon™ System (Bio-Rad), the fluorescent reporter dye SYBRGreen I (Invitrogen) and the software CFX Manager 1.6 (Bio-Rad). Reactions, primer design, controls, and PCR specificity confirmation were performed as previously described (Lara et al., 2009). Relative gene expression was estimated using the $2^{-\Delta\Delta Ct}$ method. Supplementary Table S2 shows the primers sequences used. Elongation factor 1α was employed as reference gene. Three technical replicates were run in each assay and at least three biological replicates were conducted.

2.8. Statistical analysis

Data were expressed as mean ± SD of at least three independent replicates and analyzed using One-Way ANOVA. Minimum significance differences were calculated by the Bonferroni, Holm-Sidak, Dunett, or Fisher tests ($\alpha = 0.05$) using the Sigma Stat Package.

3. Results

3.1. T. deformans detection in leaves of DOFI-84.364.060 (DR) and DOFI-84.364.089 (DS)

The first step towards the analysis of leaves from the two genotypes with contrasting susceptibility to *T. deformans* was to detect the fungus in asymptomatic leaves harvested from the experimental field, where no fungicide is applied. A representative fraction of the homogenated material was used for DNA extraction while the remaining fraction was kept at −80 °C for further analysis. The DNA obtained was subjected to PCR amplification of ITS1 region of *T. deformans* (Supplementary Fig. 1A). Amplification of ITS1 using the primers unequivocally indicates the presence of *T. deformans* in the tissue.

In all samples analyzed, the absence of putative inhibitors of amplification was tested. Using this approach all samples from the DR genotype were negative and thus indicated as DR-. Samples from the DS genotype were classified as DS+ and DS-, according to whether the 1132 bp ITS1 fragment was amplified or not. Negative samples were re-tested using different amounts of DNA (Supplementary Fig. 1B).

In addition, information regarding the phenotypic evaluation of DOFI-84.364.060 (DR) and DOFI-84.364.089 (DS) is provided (Supplementary Table S3).

3.2. Metabolomic analysis of P. persica leaves

Metabolomic profiling conducted by GC-MS allowed the identification of 67 different metabolites in *P. persica* leaves that were classified, according to their biochemical properties and functions in amino acids (19 metabolites), organic acids (15), sugars (16), sugar alcohols (5), fatty acids (2) and miscellaneous compounds (10). Metabolites were expressed in relation to the amounts in DS- (Supplementary Table S3). The metabolome of DS- leaves differs from that of DR-, and it is affected by the presence of the pathogen (DS+) (Fig. 1).

The data were subjected to principal component analysis (PCA), in which two components explain 100% of the global variance of metabolites profiles (71.83% and 28.17% for PC1 and PC2, respectively). Fig. 2 clearly depicts that the metabolome of DS is modified upon *T. deformans* infection. It also denotes that the genotypes can be separated based on their metabolite profiles.

Among the metabolites that contribute the most to PC1 are the amino acids β-Ala, Asp, Glu, Val, Asn and Ser, the fatty acid octadecanoic acid; *cis*-caffeic and galactonic acids and the sugar alcohols *myo*-inositol and maltitol; the sugars Ara, Gal, isomaltose and Xyl, and 3-*trans*-caffeoyl-quinic acid. The metabolites that contribute the most to PC2 include the amino acids His and 4-OH-

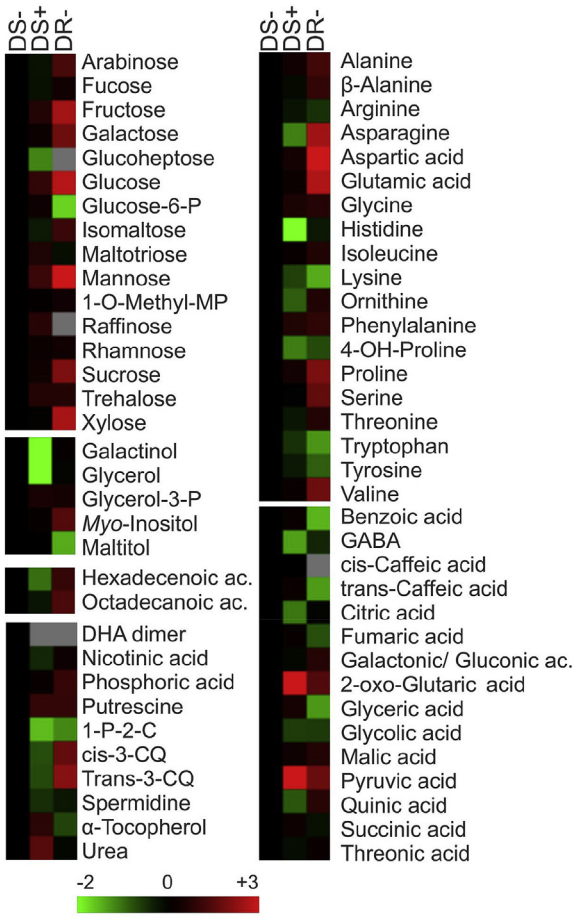

Fig. 1. Representation of metabolite profiling conducted by GC-MS. The heat map displays the relative level of each metabolite to its amount found in leaves of a susceptible genotype (DOFI-84.364.089) in which *T. deformans* was not detected (DS-) by PCR. Normalized values are shown on a color scale (shown at the bottom of the figure), which is proportional to the content of each metabolite. Values are the mean of five biological independent determinations expressed in relation to the values in DS- and expressed as log2. **DS+:** leaves of DOFI-84.364.089 positive PCR for *T. deformans* detection. **DR-:** leaves of DOFI-84.364.060 without *T. deformans* (negative PCR). Representation was generated using the MultiExperiment Viewer software (MeV v4.4.1). Relative values for each metabolite peak area ±SD are displayed in Supplementary Table S3. (For interpretation of the references to colour in this figure legend, the reader is referred to the web version of this article.)

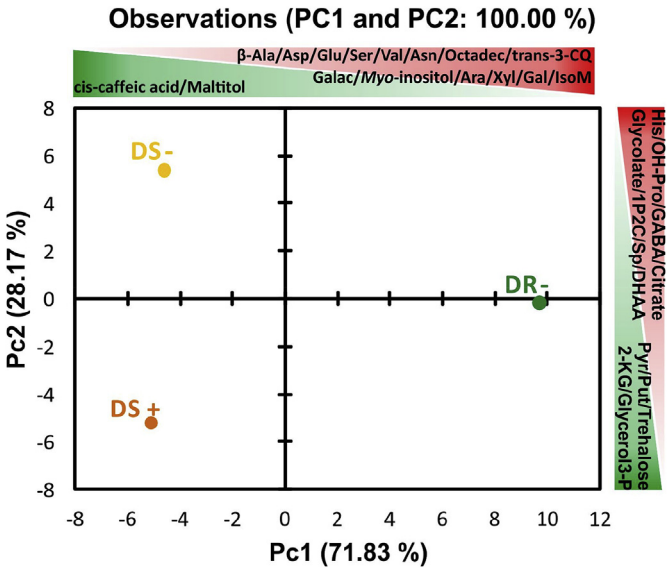

Fig. 2. Principal component analysis (PCA) of the metabolite data obtained by GC-MS. The variance explained by each component (%) is indicated in parentheses. Metabolome of leaves of the susceptible genotype DOFI-84.364.089 not infected with *T. deformans* (negative PCR, **DS-**) clearly differs from that of the resistant genotype **(DR-:** DOFI-84.364.060 not infected with *T. deformans* (negative PCR)). In leaves of the susceptible genotype in which the pathogen was detected (**DS+:** DOFI-84.364.089, positive PCR) the metabolome is reconfigured. The metabolites that contribute the most to each component are indicated on the top (PC1) and on the right (PC2). In red are shown the metabolites that positive contribute and in green those that negative contribute to each PC. 2-KG: oxo-glutarate; Put: putrescine; Octadec: Octadecanoic acid; IsoM: Isomaltose; Galact: Galactonic/Gluconic acid; Sp: Spermidine; 1P2C: 1-Pyrroline-2-carboxylate; DHAA: Dehydroascorbic acid dimer; trans-3-CQ: trans-3-caffeoyl-Quinic acid. (For interpretation of the references to colour in this figure legend, the reader is referred to the web version of this article.)

Pro, the organic acids 4-amino-butyrate (GABA), citrate, 2-oxo-glutarate, glycolate and pyruvate, glycerol 3-phosphate and trehalose and the miscellaneous compounds 1-pirroline-2-carboxylate, dehydroascorbic acid dimer, putrescine and spermidine (Supplementary Table S5).

Correlation analysis was conducted using Pearson's correlation coefficient. Among the 2211 metabolite pairs analyzed 188 resulted in significant correlation coefficients ($P < 0.05$). Of these, 125 and 63 were positive and negative, respectively (Supplementary Fig. S2). Positive correlations between sugars and most of the aminoacids were observed (except for Arg, Trp, Tyr, glucoheptose, glucose 6-phosphate). Urea and α-tocopherol negatively correlated with the majority of metabolites.

Metabolite profiling of leaves (Figs. 1 and 3, Supplementary Table S3), revealed that various amino acids (Ala, β-Ala, Asn, Asp, Glu, Ile, Phe, Pro, Ser, Thr and Val) were between 1.5- and 8.4-fold higher in the resistant (DR-) than in the susceptible genotype (DS-). On the other hand, other amino acids such as Arg, Trp and Tyr, exhibit higher relative levels in the susceptible genotype in both DS- and DS + than in the resistant. By contrast, other amino acids such as Gly, His and Orn were invariant between genotypes.

With respect to sugars, most of them (Ara, Fuc, Fru, Gal, Glc, isomaltose, Man, 1-O-methyl-mannopiranoside, Rha, Suc, trehalose and Xyl) show between two- and three-fold higher levels in DR-than in DS-. On the other hand, it is worth mentioning that while raffinose was not detected in the resistant genotype (DR-), its presence was detected in the susceptible genotype both in the presence (DS+) and absence of *T. deformans* (DS-).

In addition, with respect to the sugar alcohols glycerol and galactinol were invariant between genotypes, while maltitol in susceptible genotypes (DS+ and DS-) were three-fold higher than the levels observed in DR-. By contrast, *myo*-inositol is almost three times higher in DR with respect to DS.

Organic acids also show a differential behavior depending on the level of susceptibility to the pathogen. The relative levels of galactonate, pyruvate, quinate and 2-oxo-glutarate were higher in DR-than in DS-. By contrast, the susceptible genotype exhibits higher levels of benzoic, *trans*-caffeic, GABA, fumaric and glyceric acids. In addition, both fatty acids detected by GC-MS, were present at double the level in DR than in DS.

Regarding miscellaneous compounds, 3-*cis*- and 3-*trans*-caffeoyl-quinic acids were three-fold higher in DR-than in DS-. By contrast, the relative amounts of 1-pirroline-2-carboxylate and α-tocopherol were higher in DS-.

From the comparison between samples of the susceptible DS + *vs.* DS-, it is observed that Phe is induced in DS+ with respect to DS-. On the other hand, leaves containing *T. deformans* (DS+) show lower levels of His, Lys, 4-OH-Pro, Trp and Tyr than DS- (Figs. 1 and 3, Supplementary Table S3). While the sugars

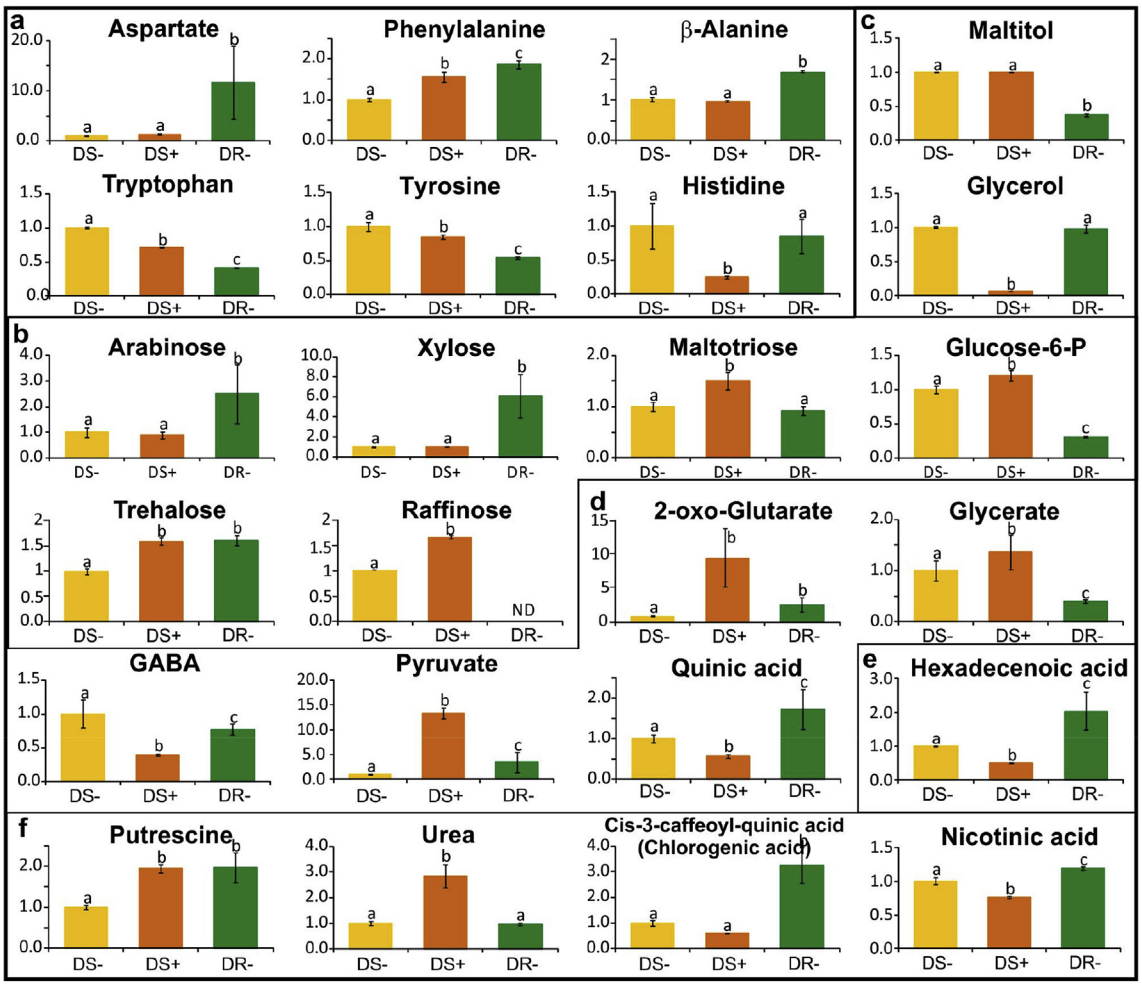

Fig. 3. Metabolite profiling conducted by GC-MS. Values represent the mean of five independent determinations using asymptomatic leaves of *P. persica*, which are expressed as the ratio with respect to DS-. Error bars represent the standard deviation. Bars with at least one same letter are not statistically different ($P < 0.05$). **DS-:** leaves of DOFI-84.364.089 in which *T. deformans* was not detected (negative PCR). **DS+:** leaves of DOFI-84.364.089 containing *T. deformans* (positive PCR). **DR-:** leaves of DOFI-84.364.060 not infected with *T. deformans* (negative PCR). **a:** aminoacids; **b:** sugars; **c:** alcohol sugars; **d:** organic acids; **e:** lipid; **f:** miscellaneous.

maltotriose, Man, raffinose and trehalose are induced in DS+ with respect to DS-, the sugar alcohols glycerol and galactinol are decreased (Figs. 1 and 3, Supplementary Table S3).

Organic acids also display the most prominent changes in PCR positive leaves; with 2-oxo-glutarate and pyruvate being ten-fold and thirteen-fold induced, respectively when the pathogen in present (DS+) whereas citrate, quinate and GABA being decreased in the same samples (Fig. 1 and Supplementary Table S3). In addition, DS + samples display lower levels of the two fatty acids detected than DS- (Fig. 1 and Supplementary Table S3).

Finally, in leaves in which *T. deformans* was detected, the relative levels of α-tocopherol, is slightly increased with respect to DS- an observation that is concordant with the carotenoid profile. Urea and putrescine are also induced in this tissue, while nicotinic acid, *cis*-3-caffeoyl-quinic acid and spermidine are repressed in DS+ with respect to DS-.

3.3. Pigment analysis

The analysis of the different leaf pigments revealed that DR- shows lower levels of chlorophylls *a* and *b*, carotenoids and anthocyanins than DS-. By contrast, DR-exhibits higher levels of total phenolic compounds than DS- (Fig. 4).

An induction of chlorophylls and carotenoids is detected in asymptomatic PCR + leaves of DS (DS+) with respect to DS-. On the other hand, total phenolics and anthocyanins decrease in the tissue with *T. deformans* (DS + *vs.* DS-, Fig. 4).

3.4. Growth inhibition curves

To test the antifungal activity of the both genotypes, leaf extracts from DR and DS plants were tested with regard to their capacity to inhibit *T. deformans* growth. Differences between genotypes were observed. While 0.5 mg/ml of DR extract was necessary to cause the 50% inhibition of fungal growth, the IC_{50} of DS was 250% higher than that of DR (Fig. 5A).

Since caffeoyl-D-quinic acid (chlorogenic acid) was higher in DR-than in both DS- and DS+, its potential role in the resistance to *T. deformans* was tested in a bioassay which gave an IC_{50} of 250 μg/ml (Fig. 5B). Dicopper chloride trihydroxide (TBCC), which is currently used in the orchards, was used as positive control (Fig. 5B).

3.5. 2-DE analysis of proteins differentially expressed between resistant and susceptible genotypes and in DS in which T. deformans is detected

Differentially expressed proteins between leaves where the

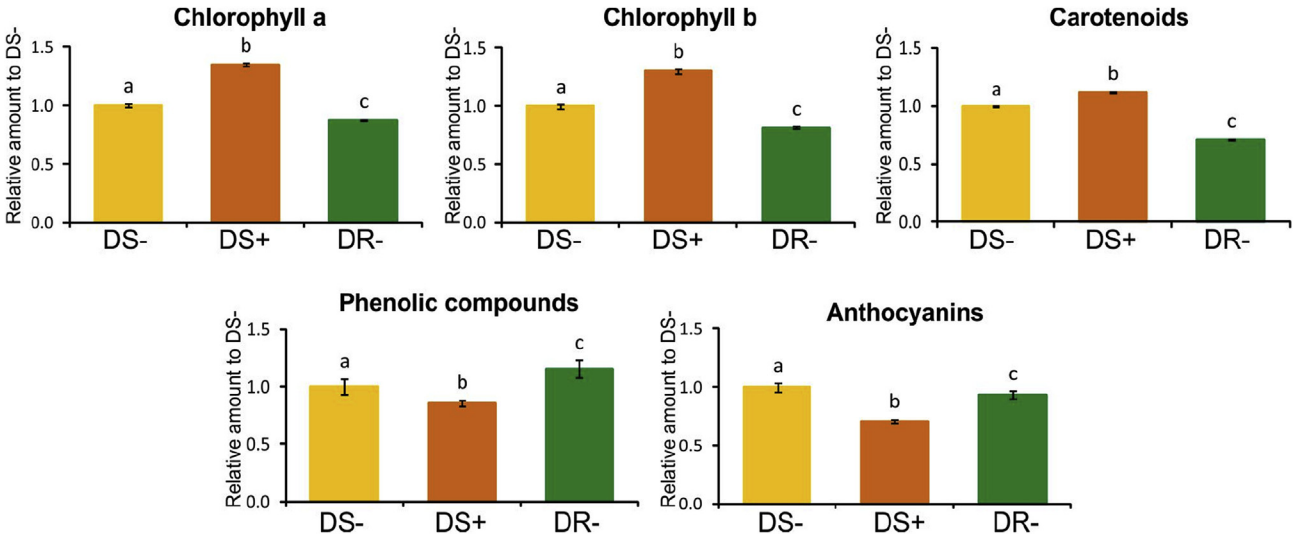

Fig. 4. Pigment content. The graph show the levels of each pigment in relation to the amount in DS-. Values represent the mean of at least three independent determinations in leaves expressed as the ratio to DS-. Error bars represent the standard deviation. Bars with at least one same letter are not statistically different ($P < 0.05$). **DS-:** leaves of DOFI-84.364.089 negative test for *T. deformans*. **DS+:** leaves of DOFI-84.364.089 with *T. deformans* (positive PCR). **DR-:** leaves of DOFI-84.364.060 free from *T. deformans* (negative PCR).

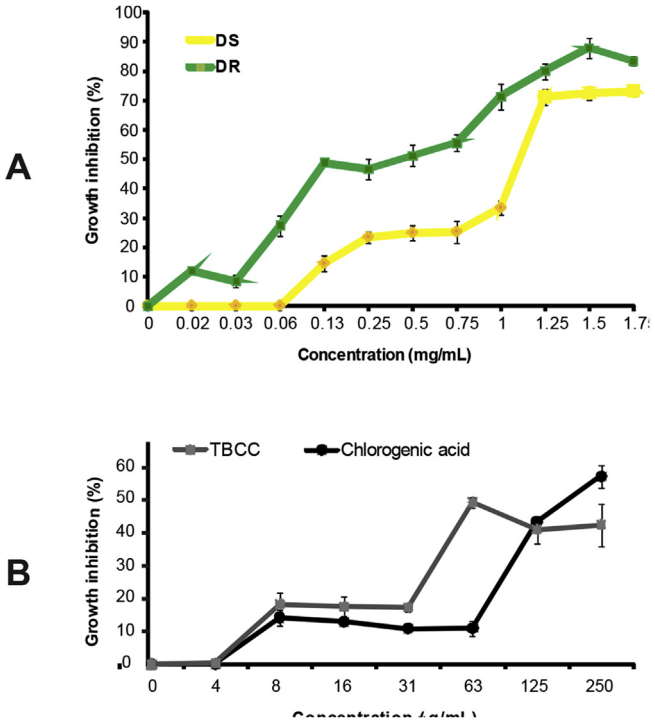

Fig. 5. *In vitro T. deformans* growth inhibition by broth microdilution technique. a. Fungal growth inhibition percentage determination of extracts of *P. persica* leaves from DS and DR genotypes. **b.** *In vitro* antifungal activity of chlorogenic acid against *T. deformans*. Dicopper chloride trihydroxide (TBCC) was used as positive control.

pathogen was not detected of the resistant (DR-) and susceptible (DS-) genotypes, and between leaves of DS where *T. deformans* was not (DS-) and was detected (DS+), were examined using 2-DE. About 400 spots were detected on each 2-DE map conducted with soluble protein from DS-, DS+ and DR- *P. persica* leaves. The left panel of Supplementary Fig. S2 shows the typical protein pattern obtained for peach leaf proteome (representative gel of protein from DS-).

Twenty four polypeptides were differentially expressed in DS- compared to DR- or DS + by a factor ±1.5 (Table 1). Twenty-one differential proteins were identified by fingerprinting mass analysis (Table 1). Missing identifications could be explained by the low abundance of the spots or the fact that the protein was not present in available databases. Among the identified spots, 71% were proteins already described in the *Prunus* spp. genus, with the majority of them (80%) already described in peach. A high proportion (67%) of the identified proteins are chloroplast localized. Differences in the analyzed proteomes included proteins involved in photosynthesis, immune and stress defense responses, protein metabolism (synthesis, folding and degradation) and redox metabolism. The significant modification in proteins related to the photosynthetic process were represented by changes in Rubisco (spots 102, 103, 104 and 224), Rubisco Activase (spot 77), triose phosphate isomerase (spots 276 and 277), and the PSII oxygen evolving enhancer protein 2 (spots 256 and 247).

Eight proteins were differentially expressed in leaves of the two genotypes in the absence of the pathogen (DR-*vs.* DS-), of which two were lower in DR-than in DS+ (spots 250 and 77), and six were only present in DR- (Table 1). The 67% of spots identified were associated with various aspects of chloroplast physiology. Among the proteins exclusively expressed in the resistant genotype, and localized to the cytosol, spot 286 is a Bet-v1-like protein involved in plant defense and spot 280 is a 2-methylene-furan-3-one reductase.

When comparing samples from the susceptible genotype free from *T. deformans* (DS-) with those in which the pathogen was detected by PCR (DS+) sixteen differential spots were identified, from which three varied their relative expression (spots 250, 22 and 47), eight were uniquely expressed after infection (DS+) and other five spots were exclusively expressed in leaves where the pathogen was not detected (DS-, Table 1). Only one spot was not identified. Some proteins such as Rubisco comprised several different spots of the same molecular mass and different isoelectric point indicating probable post-translational modification. On the other hand, various spots corresponding to different *P. persica* pathogenesis-related proteins Bet-v1-like (spots 47, 94 and 302) and others involved in protein metabolism (spots 22, 228 and 116) were detected in the comparison between DS+ and DS- 2-DE comparison.

Table 1
Identification of differentially expressed proteins as well as the trend observed in the protein abundances in *Prunus persica* leaves.

Spot N°	Fold change	MW_E (kDa)	pI_E	MW_T (kDa)	pI_T	Protein name	NCBI Accession n°	QM	Score	SC (%)	SL
DR- vs. DS-											
250	−1.59	52.4	5.5	49.9	6.1	Chloroplast elongation factor TuA (EF-TuA) [Nicotiana sylvestris]	218310	4	276	12	Chl
77	−2.27	49.6	6	48.1	5.7	Hypothetical protein PRUPE_ppa005158 mg [Prunus persica]RuBisCO activase (RCA)	596057870	10	256	23	Chl
280	+	43.9	5.7	34.4	5.4	Hypothetical protein PRUPE_ppa008712 mg [P. persica] 2-methylene-furan-3-one reductase	595938703	9	134	36	Cyt
276	+	32	5.4	38.4	8.8	Hypothetical protein PRUPE_ppa007813 mg [P. persica] Triosephosphate isomerase	595798321	6	171	17	Chl
277	+	29.1	5.4	34.1	8.2	Triosephosphate isomerase [P. mume] XP_008236196.1	645261233	3	138	12	Chl
281	+	24.4	5.7	nh	nh	no hit	–	–	–	–	–
283	+	27.6	5.8	nh	nh	no hit	–	–	–	–	–
286	+	16.6	6.2	17.3	5	Hypothetical protein PRUPE_ppa012646 mg [P. persica] Bet_v1-like	596288657	3	139	28	Cyt
DS + vs. DS-											
250	−2.54	52.4	5.5	49.9	6.1	Chloroplast elongation factor TuA (EF-TuA) [N. sylvestris]	218310	4	276	12	Chl
22	−2.36	53.9	6	52.2	6.1	Hypothetical protein PRUPE_ppa005137 mg [P. persica] 26S proteasome regulatory complex, ATPase RPT4	595823828	11	140	33	Cyt
47	4.24	18.8	5.1	17.6	5.8	Hypothetical protein PRUPE_ppa012651 mg [P. persica] Bet_v1like	596198148	7	133	45	Cyt
102	+	62.1	5.4	53.1	6.2	RuBisCO [Suriana maritima]	464024	15	104	29	Chl
103	+	62.1	5.4	53.4	6.1	RuBisCO [Typha domingensis]	218175482	17	119	32	Chl
104	+	62.1	5.3	54.3	6.5	RuBisCO [Myxopyrum hainanense]	108773686	21	123	43	Chl
224	+	62.1	6.1	53.5	6.2	RuBisCO [Guzmania vittata]	848237486	10	60	18	Chl
228	+	72.9	6.1	62	5.1	Hypothetical protein PRUPE_ppa003328 mg [P. persica] Chaperonin 60 subunit alpha1	595822952	4	69	8	Chl
116	+	25.8	5.4	26.4	7.8	Hypothetical protein PRUPE_ppa010359 mg [P. persica] 20 kDa chaperonin	595820873	4	76	11	Chl
94	+	17.5	6	17	5.2	Hypothetical protein PRUPE_ppa012809 mg [P. persica] MLP-like protein 423-related Bet_v1-like	596298706	4	91	24	Cyt
191	+	16.1	5.9	nh	nh	no hit	–	–	–	–	–
302	−	13.5	4.9	16.9	6	hypothetical protein PRUPE_ppa012870 mg [P. persica] Bet_v1-like	596198911	4	68	41	Cyt
299	−	13	5.3	15.4	5.9	PREDICTED: glutaredoxinC4 [P. mume] XP_008223820.1	645234458	5	72	42	Chl
326	−	28.5	5.2	27.5	5.8	Hypothetical protein PRUPE_ppa010431 mg [P. persica] ascorbate_peroxidase	595828925	4	116	22	Cyt
247	−	24.8	5.4	28.5	8.3	PREDICTED: oxygen-evolving enhancer protein 2 [P. mume]	645246940	6	106	33	Chl
256	−	23.8	5.7	28.6	8.3	Hypothetical protein PRUPE_ppa010093 mg [P. persica] PSII oxygenevolving enhancer protein 2 PsbP	595940575	3	215	17	Chl

Proteins were extracted from a resistant (DR-) and a susceptible genotype in which *T. deformans* was (DS+) or wasn't detected (DS-) by molecular methods. Fold change: Ratio of increase or decrease of target protein as indicated in the table. When the spot is found in only one condition of the comparison, + denotes the presence in DR-in DR-*vs.* DS-; and the presence in DS+ in DS + *vs.* DS- comparison, while − indicates the presence in DS- in both comparisons. The same meaning is giving for the + and − signs accompanying the ratios for proteins present in both samples of the comparison. MW_E: estimated molecular weight; pI_E: estimated isoelectric point; MW_T: theorical molecular weight; pI_T: theorical isoelectric point; Score: Mascot-MOWSE score; QM: Queries matched, number of peptides matched in databases; SC: sequence coverage; nh: No sequences were found in databases; SL: Subcellular localization; Chl: chloroplastic; Cyt: cytosolic.

3.6. Differences in the expression of transcripts encoding pathogenesis-related proteins

The relative expression of genes related to plant defense was evaluated by qRT-PCR and expressed in relation to the value obtained using DS- material (Fig. 6). Genes tested included: Lipid-Transfer Protein 1 (LTP1, PR14), Phenylalanine Ammonia Lyase-1 and -2 (PAL1-2), Thaumatin-Like Protein (TLP1, PR5), Catalase-1 and -2 (CAT1-2), β-1,3-endoglucanase (Gns4, PR2), Defensin 1 (DFN1, PR12) and Ribonuclease-like protein (Pp 1.06A, PR10).

On comparison of DS- with DS+, variations in mRNA levels of *PpCAT1-2*, *PpPAL1-2*, *PpLTP1*, *PpTLP1* and *PpPR10* were detected. Inductions of between 2- and 6.9- fold in leaves with vs. without *T. deformans* were recorded (Fig. 6). By contrast, there were no statistically significant differences in the relative levels of *PpGns4* and *PpDFN1*.

The comparison of transcripts levels in PCR negative leaves from the two genotypes (DS- *vs.* DR-) revealed that most of the transcripts that are induced upon *T. deformans* infection in DS (DS- *vs.* DS+) are also expressed at higher levels in DR-than in DS- and even than in DS+. This is the case for *PpCAT1*, *TpLTP1*, *PpPAL2* and *PpGns4*, which in DR-are 14.9-, 36.9-, 10.5-, and 5.9-fold higher, respectively, than in DS-. *PpPR10* accumulation in DR-is higher than in DS-, but expressed to a similar level as in DS+. In the case of *PpCAT2*, the relative levels of DR-are higher than in DS- but lower than in DS+. By contrast, *PpPAL1* transcript levels are considerably lower in DR-than in DS-. However, in the case of *PpLTP1*, there are no differences in the relative expression between the genotypes on comparison of leaves without *T. deformans* (Fig. 6).

4. Discussion

Peach leaf curl caused by *T. deformans* is one of the most important diseases of this species. In order to gain molecular level knowledge into the *P. persica* − *T. deformans* interaction two different approaches were taken. On one hand, to gain insight into the factors involved in the resistance to the disease heathy leaves free from *T. deformans* from two genotypes with contrasting susceptibility to the pathogen were compared. Two advanced selections from the self-pollinating DOFI 71.043.018 program with shared progenitors (Bellini et al., 2002) were investigated. DOFI-84.364.089 (DS) is susceptible to the pathogen, with infected trees showing typical signs of the disease. By contrast, DOFI-84.364.060 (DR) is resistant to the pathogen, with neither reddening nor leaf curl being observed across several years, even when surrounded by sick trees in the orchard. In this line, in the present work while the analysis of asymptomatic leaves of DS rendered both leaves in which the pathogen was present and those in which it was absent, that of DR was always negative. While in DR leaves inoculated with the pathogen under laboratory conditions the fungal load tend to decrease after 120 h post inoculation; in DS it greatly increased (Svetaz et al., 2017).

On the other hand, to understand the early biochemical changes that take place in leaves when the pathogen is present and the disease is not evident, leaves from the DS were contrasted when the pathogen is detected by a molecular method (DS+) with those in

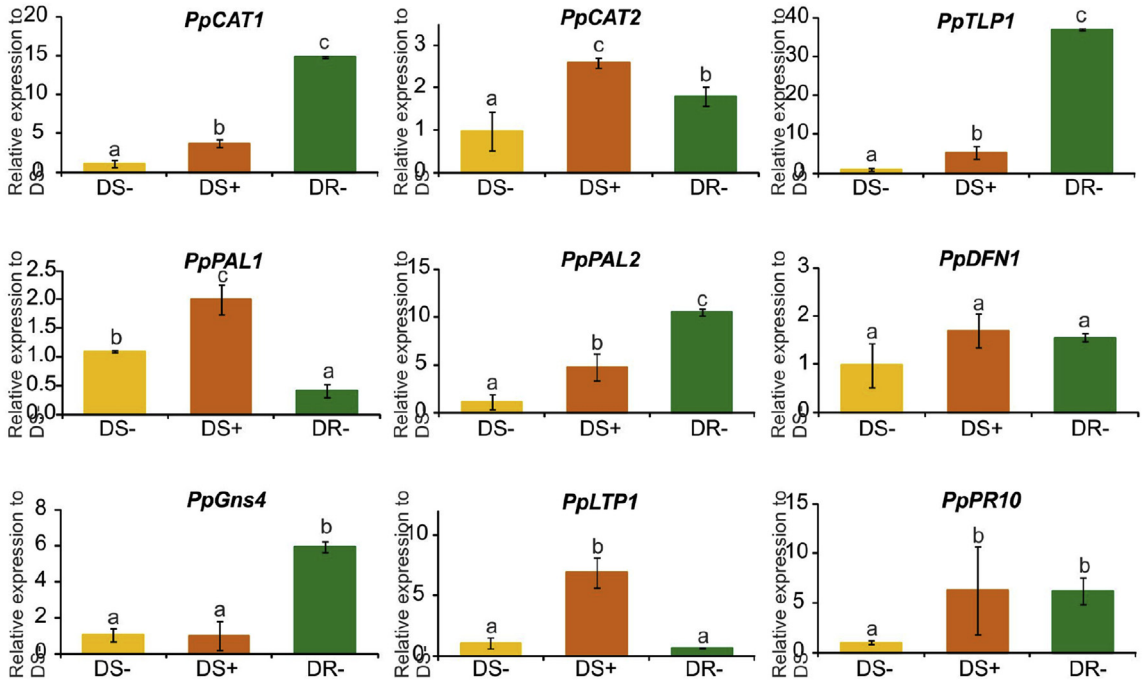

Fig. 6. Relative expression of transcripts encoding PR proteins involved in plant defense. Transcript amount was assessed by quantitative real time RT-PCR, using *P. persica* elongation factor 1α (*PpEF1α*) as reference gene. Y-axes show the fold difference in a particular transcript level relative to its amount in leaves of DOFI-84.364.089 in which *T. deformans* was not detected by molecular methods (**DS-**). Values represent the mean of at least three replicates ± SD. Bars with at least one same letter are not statistically significant ($P < 0.05$). **DS+:** leaves of DOFI-84.364.089 with *T. deformans* (positive PCR). **DR-:** leaves of DOFI-84.364.060 without *T. deformans* (negative PCR).

which the pathogen is absent (DS-).

4.1. Leaves of DR possess metabolites with anti-T. deformans activity

A considerable number of metabolites constitutively found in plants exhibit antifungal activity (Pusztahelyi et al., 2015). Phenolic compounds are included within this group. Antifungal activity of methanol extracts of the two *P. persica* genotypes against the pathogen clearly shows a differential behavior. Growth inhibition curves indicate the presence of compounds with anti-*T. deformans* properties. Part of this activity may be attributed to chlorogenic acid that is present in healthy leaves of DR-. Moreover, its inhibitory effect on *T. deformans* was demonstrated (Fig. 5B). The minimum inhibitory concentration value determined for this compound when tested on *T. deformans* was similar to values indicated in the literature for other pathogenic fungi (Sung and Lee, 2010). A strong correlation between chlorogenic acid in peach fruits and reduction in infection due to *Monilinia laxa* has been reported (Villarino et al., 2011). Preformed inhibitors may be effective against a wide range of pathogens, including *T. deformans* and *M. laxa*. Moreover, DR- shows higher accumulation of *PpPAL2* than DS-. PAL encodes the first committed step of the phenylpropanoid pathway using Phe to synthetize many metabolites involved in fungal plant defenses (Ferreira et al., 2007).

β-alanine may also contribute to *P. persica* defense. This non-protein amino acid has also been suggested to have a role in the defense response; it was only detected in elicitor-treated cultures of opium poppy cells (Zulak et al., 2008) and it was accumulated in MeJA-treated *Medicago truncatula* cells (Broeckling et al., 2005). Here, β-alanine is higher in DR-than in DS- but is not induced in the susceptible genotype when is colonized by *T. deformans*.

Trehalose is a non-reducing sugar that has a protective role in abiotic stresses. The synthesis of this disaccharide is stimulated by some plant–pathogen interactions. Nevertheless, its role in plant defense is not clear yet (Fernandez et al., 2010). On the other hand, putrescine is a polycationic amine that participates in several cellular and developmental processes, including various stress responses. Moreover, its participation in fugal resistance was demonstrated in tomato fruits (Hazarika and Rajam, 2011). In PCR negative leaves of *P. persica*, putrescine and trehalose in the resistant genotype (DR-) almost doubles the amount in the susceptible genotype (DS-), and both metabolites are induced in DS + to the same extent as in DR-, indicating that they indeed may be as part of the defense response against the pathogen.

The PCA scores plot (Fig. 2) reveals that PC1 separates the metabolome of the resistant genotype (DR-) from those of the susceptible genotype where *T. deformans* was not (DS-) and was detected (DS+). Interestingly, the maximum individual metabolite contribution to this component is 2.12%, with 31 compounds contributing in more than 2% each to PC1 and thereby accumulating a 65% contribution to this component. In other words, the contrasting profiles among metabolomes of resistant and susceptible genotypes is due to the combined composition of the whole metabolome and not to a major contribution of a few differentially abundant metabolites. Moreover, the separation of DR-from DS+ in the PCA plot reveals that DR-possess an unique profile which is not reached in DS even after the fungus is present (DS+).

4.2. Metabolome of asymptomatic DS leaves varies when T. deformans is present

The mere presence of *T. deformans* significantly affects the plant metabolic profileincluding significant modifications in the levels of amino acids, sugars, citric acid cycle intermediates and miscellaneous compounds including polyamines. This change in part reflects the induction of metabolites involved in plant defense, such as putrescine and trehalose, which are induced to the same extent

as the pre-exiting levels apparent in DR-. Additionally, it also reveals the modifications in the host cell to fuel fungal metabolism. Intriguingly more than 60% of the amino acids remained unchanged, with Phe being the only one increased, probably at expense of a decrease in Tyr in DS+. These observations are concordant with the observed induction of *PpPAL-1* and *-2* transcripts. Thus, increased Phe denotes increased flux through phenylpropanoid metabolism when *T. deformans* is present.

Interestingly, there were no significant changes in Glc, Fru or Suc, metabolites indicative of the energy status of the cell. Nevertheless, a great induction in pyruvate was observed. Moreover, the increase in maltotriose is suggestive of starch degradation, which could provide Glc to feed the energy demands required for the activation of plant defenses and/or to support fungal growth, and thus keep the homoeostasis of these sugars. In addition, the pronounced decrease in glycerol may indicate that this metabolite is being metabolized to Glycerol 3-P and then to dihydroxyacetone phosphate to fuel glycolysis, resulting in the increased pyruvate detected. Moreover, the slight increase in Glc 6-P suggests stimulation of pentose phosphate pathway to produce reductive power to be used by NADPH oxidases at the plasma membrane as well as in the cell-wall fortification (Scheideler et al., 2002). On one hand, both glycolytic and pentose phosphate pathways influence the shikimic pathway; and thus, its derivatives. On the other hand, and in agreement with the increased levels of chlorophylls and carotenoids, the higher levels of pyruvate in DS+, may be used together with glyceraldehyde 3-phosphate to fuel the isoprenoid biosynthesis in the chloroplast using the non-mevalonate pathway (Vranova et al., 2012). Furthermore, in symptomatic leaf curl an increase in isopentenyltransferase involved in zeatin synthesis was recorded and related to the hyperplasia typical of the disease (Testone et al., 2008). Thus, in the asymptomatic leaves analyzed here, increased flux thought this pathway might also fuel cytokinin biosynthesis.

The increase 2-oxo-glutarate in DS+ in comparison with DS- is worth of mention. It is surprising that this metabolite is the only Krebs cycle intermediate induced in the presence of *T. deformans*. However, further research is likely needed to explain the reason for this specific change.

The induction of raffinose in DS+ with respect to DS- is statistically significant, and in agreement with the decrease in its precursor, galactinol. Although in some cases, raffinose accumulation was proposed to act as a signaling molecule for defense (ElSayed et al., 2013); here, it is remarkable that raffinose was not detected in leaves of the resistant genotype (DR-) thus rather supporting the hypothesis that this trisaccharide serves as nutrition for the fungi. Given that the genome of the pathogen encodes a SIP2 enzyme putatively involved in raffinose degradation (TAPDE_002196g.01; http://genome.jgi.doe.gov/pages/search-for-genes.jsf?organism=Tapde1_1), provides further support for this theory.

Finally, urea could act as a nitrogen source for *T. deformans* since a distinctive feature of this fungus is its urease activity (Fonseca and Rodrigues, 2011).

4.3. Proteome analysis reveals the chloroplast to be an important site of plant defense responses and differential behavior of Bet-v1-like proteins against T. deformans

Numerous studies have shown the benefits of the proteomics approach for elucidating underlying plant defense response (Mehta et al., 2008). The current work is, however, the first comparative proteomic study regarding the *P. persica-T. deformans* interaction.

Among proteomic changes observed, photosynthesis seems to be majorly affected in leaves with the pathogen. Up-regulation of Rubisco (spots 102–104, 224) agrees with rises in chlorophylls and carotenoids, which are structural components of PSI and PSII reaction center complexes also measured in the asymptomatic phase. Nevertheless, decreases in a putative PSII oxygen evolving enhancer protein II (spots 247, 256) were also detected. Metabolomics studies revealed that sugars such as Fru, Glc or Suc are not affected in this asymptomatic stage of the infection and suggest that modifications at protein and pigment levels are enough to maintain photosynthetic products homeostasis. During early stages of naturally occurring infection (in the asymptomatic phase), there are increased demands for resources to support defense and thus photosynthesis may be enhanced. As the disease progresses, there is a reduction of photosynthetic capacity, as accounted by a net decrease in carbon fixation and a moderate decrease in the photochemical reactions in symptomatic curled leaves (Raggi, 1995).

Chloroplast protein control, through the activities of elongation factor Tu (EF-Tu, spot 250) and chaperonins (spots 228 and 216), is involved in the response or homeostasis against *T. deformans*. Besides its role in peptide elongation, chloroplast EF-Tu plays an important function in heat tolerance, acting as a molecular chaperone in maize (Ristic et al., 2007), whilst abiotic factors and hormones regulate it in pea. EF-Tu was depressed and interacted with leucine-rich repeat receptor-like kinases in Chinese cabbage following infection with turnic mosaic virus (Peng et al., 2014). The high proportion of proteins localized to the chloroplast that change upon *T. deformans* infection reveals the function of this organelle is crucial to defense responses against the pathogen. Location of most of the differentially expressed proteins in DR-*vs.* DS- indicates that chloroplast proteome may be important in the resistance. For example, portions of jasmonic and salicylic acid biosynthesis occur at the chloroplasts (Acosta et al., 2009; Chen et al., 2009), whilst precursors of cytokinins, related to disease symptoms, are also synthesized in the chloroplast (Sakakibara, 2006).

Bet-v1 is the main allergen of the birch (*Betula verrucosa*, Bufe et al., 1996). Homologues to this protein are found not only in pollen but also in latex and fruits (Vanek-Krebitz et al., 1995; Scheurer et al., 1997). These proteins possess a common β-α2-β6-α fold, the "Bet v1-like fold", and are homologues to the PR10 family. Regardless of the immunological importance of Bet-v1 and Bet-v1-like proteins, little is known about their biological role. While some members possess RNase activity, others bind ligands such as homocastasterone, fatty acids and cytokinins (Mogensen et al., 2002). This last binding capacity could be of relevance since cytokinins enhanced production is related to disease symptoms of hyperplasia (Testone et al., 2008). Many Bet-v1 proteins show enhanced expression during disease and/or stress situations (Gupta et al., 2015). Here, several of the differentially expressed proteins correspond to Bet-v1-like family and show variable response against the pathogen. Spot 286 (ppa012646 mg) may be related to resistance against *T. deformans*. Moreover, *PpPR10* (ppa012627m) analyzed at transcriptional level also belong to the same family and it is accumulated to the same extent in both DS+ and in healthy leaves of the resistant genotype (DR-). Therefore, the diverse members of the family exhibit a differential behavior against the pathogen; while some may function as pre-formed defense proteins against a broad range of pathogens, after challenge with *T. deformans* those specifically involved in the defense against this fungus are increased, or even *de novo* synthesized, while others are repressed.

Interestingly, the differential proteome of resistant *vs.* susceptible genotypes identified a putative 2-methylene-furan-3-one reductase (spot 280). In strawberry, this protein is a ripening-induced, negatively auxin-regulated enzyme (Schiefner et al., 2013). Different furanones present antifungal activity against plant pathogens such as *Pythium ultimum*, *Fusarium solani* and

Thielaviopsis basicola (Paulitz et al., 2000). Here, exclusive occurrence of the reductase in DR-may produce volatiles contributing to *T. deformans* resistance.

4.4. *P. persica* pathogenesis-related proteins play a role in the defense against *T. deformans*

Pathogenesis-related proteins (PRs) comprise a large group of proteins with significant function in induced and in some cases constitutive resistance. According to their biochemical and biological features, they are grouped within 17 families (van Loon et al., 2006). Results obtained at the protein level were discussed above; the transcriptional analysis is discussed below. Thaumatin-like proteins (TLPs, PR5) are proposed to act as antifungal by creating pores in the plasma membrane of the pathogen increasing its permeability (Koiwa et al., 1997). In the pathosystem under study, *PpTLP1* is induced upon infection and its presence in a greater magnitude in DR-than in both DS- and DS- reveals its relevant role in fighting against *T. deformans*.

β-Glucanases (PR2) have diverse activity and localization (Simmons, 1994). *PpGns4* is a 1,3-β-D-glucanase expressed at higher levels in DR-than in DS- which may also contribute to the resistance of DR-. This could be an effective mechanism against *T. deformans*, considering its cell wall contains a 60–70% of β-glucanes and chitin only represents less than 2‰ of cell wall (Petit and Schneider, 1983).

Lipid-Transfer Proteins (LTPs) are antibacterial and antifungal peptides formerly assumed, yet currently considered unlikely, to participate in intracellular lipid trafficking (Yeats and Rose, 2008). In *P. persica, PpLTP1* is accumulated in the epicarp of fruits challenged with *Monilia* (Botton et al., 2002). Here, *PpLTP1* is more abundant in leaves in the presence of the pathogen than in its absence. By contrast to *PpGns4* and *PpTLP1,* there are no differences in *PpLTP1* levels between leaves of both genotypes in which the pathogen is not detected.

Bioinformatic analysis (Supplementary Table S6) reveals PpGns4, PpTLP1 and PpLTP1 putative proteins are likely to be extracellular. Given that *T. deformans* hyphal growth takes place in intracellular spaces and between cuticle and epidermal cells, the presence of PpGns4, PpTLP1, PpLTP1 in this location would be of relevance for fungal cell wall degradation, thus increasing the permeability of the pathogen and providing a mechanism to combat *T. deformans* and/or confer resistance to it.

5. Conclusions

Disease resistance in plant depends on complex integrated mechanisms. In *P. persica* resistance against *T. deformans* is a polygenic trait mediated by several factors. Here, some protective compounds and proteins such as chlorogenic acid, furanones, PpGns4, PpTLP1 and Bet-v1-like proteins are constitutively present in leaves of resistant peach trees. Since many of these preformed antimicrobial compounds and proteins are effective in plant defense against other pathogens, in future studies it would be interesting to test the response of the resistant genotype against other pathogens of economic importance such as *M. laxa*. Moreover, the DOFI-84.364.060 genotype analyzed in this work could be used in future breeding programs as a source of *T. deformans'* resistance to improve already commercial cultivars that exhibit satisfactory yields, produce fruit of quality and are adapted to different climatic conditions. On one hand, accessibility of cultivars that are tolerant to the pathogen is key to reduce losses in production and money invested in fungicides. On the other hand, there is an environmental benefit, avoiding negative impacts on human and livestock health and diminishing the risks of pathogen resistance due to the use of pesticides. This study also explored the defense mechanisms operating in susceptible trees. In asymptomatic leaves in which *T. deformans* was detected, some defense mechanisms are activated, such as an induction of catalase, PAL and PR proteins. Nevertheless, they exhibit altered primary metabolism and modification of photosynthetic apparatus components, revealing that induced defenses are not sufficient to fully counteract the fungal attack.

Contributions

CG, LAS, CAB and MA conducted the experiments. GHV grew the trees, monitored the plants, selected, and collected the material.

MFD and ARF interpreted experimental data and revised the manuscript. MVL conceived the study, analyzed and interpreted the data and wrote the manuscript. All of the authors read and approved the final manuscript.

Acknowledgments

LAS, CAB, MFD and MVL are CONICET Researcher Career members. CAB received an Alexander von Humboldt Foundation fellowship at ARF lab. We thank Professors Bellini and Giordani (DISPAA, Università di Firenze) for *P. persica* selections.

This work was supported by Agencia Nacional de Promoción Científica y Tecnológica (PICT 2012-1376). INTA supported the *P. persica* collection (PNFRU 1105062; REDGEN 1137021; PReT 127128).

Appendix A. Supplementary data

Supplementary data related to this article can be found at http://dx.doi.org/10.1016/j.plaphy.2017.06.022.

References

Acosta, I., Laparra, H., Romero, S.P., Schmelz, E., Hamberg, M., Mottinger, J.P., Moreno, M.A., Dellaporta, S.L., 2009. *tasselseed1* is a lipoxygenase affecting jasmonic acid signalling in sex determination of maize. Science 323, 262–265.

Arús, P., Verde, I., Sosinski, B., Zhebentyayeva, T., Abbott, A.G., 2012. The peach genome. Tree Gen. Genom 8, 531–547.

Bassi, M., Conti, G.G., Barbieri, N., 1984. Cell wall degradation by *Taphrina deformans* in host leaf cells. Mycopathologia 88, 115–125.

Bellini, E., Giordani, E., Perria, R., Paffetti, D., 2002. Leaf curl in peach: new resistant genotypes and molecular markers. Acta Hortic. 592, 649–653.

Botton, A., Begheldo, M., Rasori, A., Bonghi, C., Tonutti, P., 2002. Differential expression of two lipid transfer protein genes in reproductive organs of peach (*Prunus persica* L. Batsch). Plant Sci. 163, 993–1000.

Broeckling, C.D., Huhman, D.V., Farag, M.A., Smith, J.T., May, G.D., Mendes, P., Dixon, R.A., Sumner, L.W., 2005. Metabolic profiling of *Medicago truncatula* cell cultures reveals the effects of biotic and abiotic elicitors on metabolism. J. Exp. Bot. 56, 323–336.

Bufe, A., Spangfort, M.D., Kahlert, H., Schlaak, M., Becker, W.-M., 1996. The major birch pollen allergen, Bet v. 1, shows ribonuclease activity. Planta 199, 413–415.

Casati, P., Zhang, X., Burlingame, A.L., Walbot, V., 2006. Analysis of leaf proteome after UV-B irradiation in maize lines differing in sensitivity. Mol. Cel. Proteomics 4.11, 1673–1685.

Chase, M., Fay, M., 2009. Barcoding of plants and fungi. Science 325, 682–683.

Chen, Z., Zheng, Z., Huang, J., Lai, Z., Fan, B., 2009. Biosynthesis of salicylic acid in plants. Plant Signal. Behav. 4, 493–496.

ElSayed, A.I., Rafudeen, M.S., Golldack, D., 2013. Physiological aspects of raffinose family oligosaccharides in plants: protection against abiotic stress. Plant Biol. 16, 1–8.

Fernandez, O., Bethencourt, L., Quero, A., Sangwan, R.S., Clement, C., 2010. Trehalose and plant stress responses: friend or foe? Trends Plant Sci. 15, 409–417.

Fernie, A.R., Aharoni, A., Willmitzer, L., Stitt, M., Tohge, T., Kopka, J., et al., 2011. Recommendations for reporting metabolite data. Plant Cell 23, 2477–2482.

Ferreira, R.B., Montero, S., Freitas, R., Santos, C.N., Chen, Z., Batista, L.M., Duarte, J., Borges, E., Teixeira, A.R., 2007. The role of plant defence proteins in fungal pathogenesis. Mol. Plant Pathol. 8, 667–700.

Fonseca, A., Rodrigues, M.G., 2011. *Taphrina* fries. Chapter 73. In: Kurtzman, C.P., Fell, J.W., Boekhout, T. (Eds.), The Yeasts, a Taxonomic Study, fifth ed. Elsevier, The Netherlands, pp. 823–858.

Giordani, E., Giuseppe, P., Raddice, S., 2013. Compared anatomy of young leaves of *Prunus persica* (L.) Batsch with different degrees of susceptibility to *Taphrina*

deformans (Berk.) Tul. J. Phytopathol. 161, 190–196.
Giosuè, S., Spada, G., Rossi, V., Carli, G., Ponti, I., 2000. Forecasting infections of the leaf curl disease on peaches caused by *Taphrina deformans*. Eur. J. Plant Pathol. 106, 563–571.
Gupta, S., Wardhan, V., Kumar, A., Rathi, D., Pandey, A., Chakraborty, S., Chakraborty, N., 2015. Secretome analysis of chickpea reveals dynamic extracellular remodeling and identifies a Bet v1-like protein, CaRRP1 that participates in stress response. Sci. Rep. 5, 18427.
Hazarika, P., Rajam, M.V., 2011. Biotic and abiotic stress tolerance in transgenic tomatoes by constitutive expression of S-adenosylmethionine decarboxylase gene. Physiol. Mol. Biol. Plants 17, 115–128.
Koiwa, H., Kato, H., Nakatsu, T., Oda, J., Yamada, Y., et al., 1997. Purification and characterization of tobacco pathogenesis-related protein PR-5d, an antifungal thaumatin-like protein. Plant Cell Physiol. 38, 783–791.
Lara, M.V., Borsani, J., Budde, C.O., Lauxmann, M.A., Lombardo, V.A., Murray, R., Andreo, C.S., Drincovich, M.F., 2009. Biochemical and proteomic analysis of "Dixiland" peach fruit (*Prunus persica*) upon heat treatment. J. Exp. Bot. 60, 4315–4333.
Mehta, A., Brasileiro, A.C., Souza, D.S., Romano, E., Campos, M.A., Grossi-de-Sá, M.F., et al., 2008. Plant-pathogen interactions: what is proteomics telling us? FEBS J. 275, 3731–3746.
Mogensen, J.E., Wimmer, R., Larsen, J.N., Spangfort, M.D., Otzen, D.E., 2002. The major birch allergen, Bet v 1, shows affinity for a broad spectrum of physiological ligands. J. Biol. Chem. 277, 23684–23692.
Monti, L.L., Bustamante, C.A., Osorio, S., et al., 2016. Metabolic profiling of a range of peach fruit varieties reveals high metabolic diversity and commonalities and differences during ripening. Food Chem. 190, 879–888.
Paulitz, T., Nowak-Thompson, B., Gamard, P., Tsang, E., Loper, J., 2000. A novel antifungal furanone from *Pseudomonas aureofaciens*, a biocontrol agent of fungal plant pathogens. J. Chem. Ecol. 26, 1515–1524.
Padula, G., Bellini, E., Giordani, E., Ferri, A., 2008. Further investigations on the resistance to leaf curl (*Taphrina deformans* Berk. Tul.) of peach cultivars and F1 progenies. In: Di Vaio, C., Damiano, C., Fideghelli, C. (Eds.), Atti del VI Convegno Nazionale Sulla Peschicoltura Meridionale. Imago Media Editrice, Dragoni, pp. 13–119.
Peng, H.-T., Li, Y.-X., Zhang, C.-W., Li, Y., Hou, X.-L., 2014. Chloroplast elongation factor BcEF-Tu responds to turnip mosaic virus infection and heat stress in non-heading Chinese cabbage. Biol. Plant. 58, 561–566.
Petit, M., Schneider, A., 1983. Chemical analysis of the wall of the yeast form of *Taphrina deformans*. Arch. Microbiol. 135, 141–146.
Pusztahelyi, T., Holb, I.J., Pócsi, I., 2015. Secondary metabolites in fungus-plant interactions. Front. Plant Sci. 6, 573.
Raggi, V., 1995. CO_2 assimilation and chlorophyll fluorescence in peach leaves affected by *Taphrina deformans*. Physiol. Plantarum 93, 5440–5444.
Rex, J.H., Alezander, B.D., Andes, D., et al., 2008. Clinical and Laboratory Standards Institute, Reference Method for Broth Dilution Antifungal Susceptibility Testing of Yeasts, Approved Standard (CLSI Document M27-A3), third ed., vol. 28. Clinical and Laboratory Standards Institute; NCCLS, Wayne, PA, pp. 1–25.
Ristic, Z., Momcilovic, I., Fu, J., Callegari, E., DeRidder, B.P., 2007. Chloroplast protein synthesis elongation factor, EF-Tu, reduces thermal aggregation of rubisco activase. J. Plant Physiol. 164, 1564–1571.
Roessner-Tunali, U., Hegemann, B., Lytovchenko, A., Carrari, F., Bruedigam, C., Granot, D., Fernie, A.R., 2003. Metabolic profiling of transgenic tomato plants overexpressing hexokinase reveals that the influence of hexose phosphorylation diminishes during fruit development. Plant Physiol. 133, 84–99.
Rossi, V., Bolognesi, M., Languasco, L., Giosuè, S., 2006. Influence of environmental conditions on infection of peach shoots by *Taphrina deformans*. Phytopathology 96, 155–163.
Rossi, V., Bolognesi, M., Giosuè, S., 2007. Influence of weather conditions on infection of peach fruit by *Taphrina deformans*. Phytopathology 97, 1625–1633.
Sakakibara, H., 2006. Cytokinins: activity, biosynthesis, and translocation. Ann. Rev. Plant Biol. 57, 431–449.
Sampaio, J.P., Gadanho, M., Santos, S., Duarte, F.L., Pais, C., Fonseca, A., Fell, J.W., 2001. Polyphasic taxonomy of the basidiomycetous yeast genus *Rhodosporidium: R. ratochvilovae* and related anamorphic species. Int. J. Syst. Evol. Microbiol. 51, 687–697.
Scheideler, M., Schlaich, N.L., Fellenberg, K., Beissbarth, T., Hauser, N.C., Vingron, M., Slusarenko, A.J., Hoheisel, J.D., 2002. Monitoring the switch from housekeeping to pathogen defence metabolism in *Arabidopsis thaliana* using cDNA arrays. J. Biol. Chem. 277, 10555–10561.
Scheurer, S., Metzner, K., Haustein, D., Vieths, S., 1997. Molecular cloning, expression and characterization of Pru a 1, the major cherry allergen. Mol. Immunol. 34, 619–629.
Schiefner, A., Sinz, Q., Neumaier, I., Schwab, W., Skerra, A., 2013. Structural basis for the enzymatic formation of the key strawberry flavor compound 4-hydroxy-2,5-dimethyl-3(2H)-furanone. J. Biol. Chem. 288, 16815–16826.
Scorza, R., 1992. Evaluation of foreign peach and nectarine introductions in the U.S. for resistance of leaf curl [*Taphrina deformans* (Berk.) Tul.]. Fruit. Var. J. 46, 141–145.
Shulaev, V., Korban, S.S., Sosinski, B., et al., 2008. Multiple models for Rosaceae genomics. Plant Physiol. 147, 985–1003.
Simeone, A.M., 1987. Osservazioni su alcuni caratteri morfologici e sulla sensibilita del pesco (*Prunus persica* vulgaris Stokes) alla *Sphaerotheca pannosa* (Wallr.: Fr.) Lev. e alla *Taphrina deformans* (Berk.) Tul. Inf. Fitopatol. 7–8, 71–76.
Simmons, C.R., 1994. The physiology and molecular biology of plant 1,3-β-D-glucanases and 1,3;1,4-β-D-glucanases. Crit. Rev. Plant Sci. 13, 325–387.
Sung, W.S., Lee, D.F., 2010. Antifungal action of chlorogenic acid against pathogenic fungi, mediated by membrane disruption. Pure Appl. Chem. 82, 219–226.
Svetaz, L.S., Bustamante, C.A., Goldy, C., Rivero, N., Müller, G.L., Valentini, G.H., Fernie, A.R., Drincovich, M.F., Lara, M.V., 2017. Unraveling early events in the *Taphrina deformans* – *Prunus persica* interaction: an insight into the differential responses in resistant and susceptible genotypes. Plant Cell Environ. http://dx.doi.org/10.1111/pce.12942.
Tavares, S., Inácio, J., Fonseca, A., Oliveira, C., 2004. Direct detection of *Taphrina deformans* on peach trees using molecular methods. Eur. J. Plant Pathol. 110, 973–982.
Testone, G., Bruno, L., Condello, E., et al., 2008. Peach [*Prunus persica* (L.) Batsch] KNOPE1, a class 1 KNOX orthologue to Arabidopsis BREVIPEDICELLUS/KNAT1, is misexpressed during hyperplasia of leaf curl disease. J. Exp. Bot. 59, 389–402.
Vanek-Krebitz, M., Hoffmann-Sommergruber, K., Laimer da Camara Machado, M., Susani, M., Ebner, C., Kraft, D., Scheiner, O., Breiteneder, H., 1995. Cloning and sequencing of Mal d 1, the major allergen from apple (*Malus domestica*), and its immunological relationship to Bet v 1, the major birch pollen allergen. Biochem. Biophys. Res. Commun. 214, 538–551.
van Loon, L.C., Rep, M., Pieterse, C.M., 2006. Significance of inducible defense-related proteins in infected plants. Annu. Rev. Phytopathol. 44, 135–162.
Villarino, M., Sandin-España, P., Melgarejo, P., De Cal, A., 2011. High chlorogenic and neochlorogenic acid levels in immature peaches reduce *Monilinia laxa* infection by interfering with fungal melanin biosynthesis. J. Agr. Food Chem. 59, 3205–3213.
Vranova, E., Coman, D., Gruissemn, W., 2012. Structure and dynamics of the isoprenoid pathway network. Mol. Plant 5, 318–333.
Yeats, T.H., Rose, J.K.C., 2008. The biochemistry and biology of extracellular plant lipid-transfer proteins (LTPs). Protein Sci. 17, 191–198.
Zhivondov, A., Dabov, S., Bozhikov, Y., 2016. 'Evmolpiya' - a new Bulgarian peach cultivar resistant to leaf curl disease (*Taphrina deformans*). Acta Hortic. 1139, 67–70.
Zulak, K.G., Weljie, A.M., Vogel, H.J., Facchini, P.J., 2008. Quantitative ^{1}H NMR metabolomics reveals extensive metabolic reprogramming of primary and secondary metabolism in elicitor-treated opium poppy cell cultures. BMC Plant Biol. 8, 5.